Optical Kerr Nonlinear Performance of Metal-Cap Wedged-Shape Hybrid Plasmonic Waveguide

Hossein Rahimi[1], Mahmoud Nikoufard[2]*, Mojtaba Dehghani Firouzabadi[3]
1- Department of Electrical Engineering, , College of Technical, Khomein Branch, Islamic Azad University, Khomein, Iran.
2- Department of Electronics, Faculty of Electrical and Computer Engineering, University of Kashan, Kashan, Iran.
E-mail: mnik@kashanu.ac.ir (Corresponding author)
3- Department of Electrical Engineering, Arak Branch, Islamic Azad University, Arak, Iran.

Received: 10 December 2022 Revised: 2 January 2023 Accepted: 14 February 2023

ABSTRACT:
This paper aims to investigate the enhancement of Kerr nonlinear performance caused by more optical confinement and longer propagation length due to different metal-cap wedge-shaped hybrid plasmonic waveguide geometric parameters. In this work, we will focus on Kerr nonlinear effect, and analyze how the different waveguide geometries can enhance this effect. Our theoretical investigation shows that the presented nonlinear wedge-shaped hybrid plasmonic waveguide structure with a wedge-shaped gap is suitable for photonic integrated circuits based on the hybrid plasmonic passive waveguide, and is a suitable candidate for the photonic devices at nano-scales with nonlinearity. It is also found that the investigated structure can have a longer propagation length of 2120 μm at a 10 nm thick nonlinear dielectric. The minimum effective mode area of the investigated structure is 0.0263 μm^2 and the maximum nonlinear coefficient is $\gamma = 3.5 \times 10^6 W^{-1}Km^{-1}$. Also, the confinement factor of the DDMEBT layer is calculated by changing the wedge angle α. It is found that the surface mode has a maximum confinement factor of 0.33 when $\alpha = 35°$. The modal and nonlinear properties of the hybrid plasmonic waveguides were analytically determined as well by using the finite element method (FEM). Simulation results show that the wedge-shaped hybrid plasmonic waveguide provides good performance for nonlinear applications such as optical switching at the optical wavelength of $\lambda = 1550$ nm.

KEYWORDS: Plasmonic, Kerr Effect, Wedge Shape, Nonlinear Coefficient, Effective Area, Confinement Factor, Fig. of Merit.

1. INTRODUCTION

Hybrid plasmonic waveguides (HPW) are passive photonic structures in which a dielectric with a low refractive index separates a metal cap layer and a high refractive index material [1]. These structures provide low propagation losses, while still having strong mode confinement. Hybrid plasmonic waveguides can be implemented on an SOI platform in form of a metal cap on a silicon (Si) rib or strip [2, 3]. The mode is predominantly confined in the gap layer with some residual field in the silicon core. Generally, with increasing gap thickness, the mode becomes more photonic with lower propagation losses.

One of the ultra-fast nonlinear effects is the Kerr effect, which is commonly used for optical switching. The Kerr effect was described by a change in refractive index proportional to the intensity of light [4]. Surface plasmon polaritons (SPPs) are attractive for switching applications because the strong local electric fields help induce nonlinear processes [5]. Additionally, SPPs are very sensitive to changes of the refractive index of the dielectric medium [6]. The wedge plasmonic waveguide (WPW) is a good candidate for achieving large degrees of confinement and high propagation lengths [7]. The wedge-shaped waveguide consists of a high refractive index material with a triangular tip caped with a thin and low refractive index layer and a noble metal on top. The wadge-shaped waveguide cross-sections were simulated by three parameters, including the slot height, the tip angle (α), and the ridge width. In comparison with the planar hybrid plasmonic waveguide, the wedge-shaped type requires more complex fabrication process and these three parameters allows further control of the plasmon polariton propagation and improving optical field capabilities. In addition, a focused-ion beam [8] and high-quality photolithography [9] procedures have been previously utilized for the fabrication of wedge-shaped waveguide, though more technological

Paper type: Research paper
DOI: 10.30486/mjtd.2023.1977581.1015
How to cite this paper: H. Rahimi, M. Nikoufar and M. Dehghani Firouzabadi, "**Optical Kerr Nonlinear Performance of Metal-Cap Wedged-Shape Hybrid Plasmonic Waveguide**", *Majlesi Journal of Telecommunication Devices*, Vol. 12, No. 1, pp. 29-35, 2023.

enhancements are required to perform complex photonic circuits [10].

The optical Kerr effect has a main role in nonlinear integrated photonics, which utilizes high-power semiconductor lasers. It is one of the essential mechanisms to generate picosecond optical pulses. Some of the application areas of the nonlinear Kerr effect include digital photography to create a type of shutter with very short exposures and rapid reaction, and photonic devices [11, 12].

In this paper, a metal-cap wedge-shaped hybrid plasmonic waveguide is presented and the effects of various geometric parameters on the Kerr performance are analyzed at an optical communication wavelength of 1550 nm. This theoretical analysis mainly investigates the nonlinear response which depends on the nonlinear coefficient (γ), propagation length (L_P), optical confinement (Γ), and Fig. of merit (FoM).

2. NONLINEAR WEDGE-SHAPED HYBRID PLASMONIC WAVEGUIDE STRUCTURE

Fig. 1 shows the cross-section of the investigated structure, which is similar to the one reported in [7] with a nonlinear polymer between silicon and a metallic layer. The width and height of the nonlinear polymer layer are $W$and h_{gap}, respectively. The considered polymer is DDMEBT (2-[4-(dimethylamino)phenyl]-3-f[4- (dimethylamino)phenyl]ethynylgbuta-1,3-diene-1,1,4,4- tetracarbonitrile) with a refractive index of n = 1.8 and nonlinear index of $n_2 = 1.7 \times 10^{-17}\text{m}^2\text{W}^{-1}$at the wavelength of 1550 nm [13, 14]. The metal layer is silver (Ag) due to its relatively low loss in the simulation wavelength. The value of the refractive index for Si and SiO2 are 3.4 and 1.45, respectively, and the refractive index of silver is equal to 0.144+11.366i [15, 16] at the operating wavelength. In addition, the nonlinear index for Si is $n_2 = 2.5 \times 10^{-18}\text{m}^2\text{W}^{-1}$ and $n_2 = 3.2 \times 10^{-20}\text{m}^2\text{W}^{-1}$ for SiO_2.

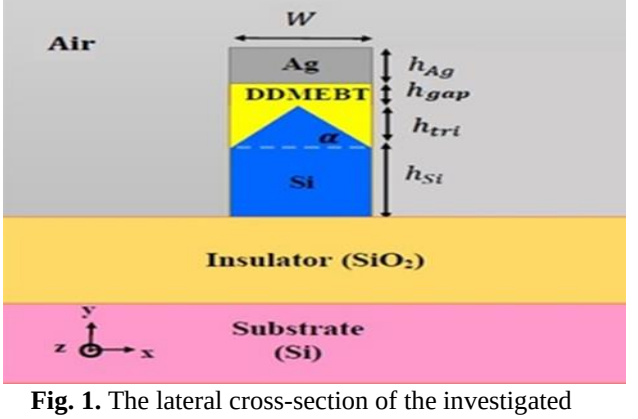

Fig. 1. The lateral cross-section of the investigated NWHPW. The thickness of Ag, DDMEBT, and Si layers are 〖h〗_Ag, h_gap 〖,h〗_tri, and h_Si, respectively.

The silicon core was fixed to a height of h_Si=200 nm nm and a width W=200 nm. The thickness of the metal film h_Ag=110nm and h_tri=W/2 tan⁡α determined by W and α. Fig.2 shows the corresponding electrical field distribution of the TM fundamental mode in the nonlinear wedge-shaped hybrid plasmonic waveguide (NWHPW) for h_gap=10nm at a wavelength of 1550 nm, determined using the COMSOL software. The optical field is predominantly confined in the DDMEBT gap with some residual field in the silicon core.

Fig. 2 also shows the 1D plots of the y-component of the electrical field of fundamental mode at the two cross-sectional of the waveguide. The electrical field is highly focused in the nonlinear DDMEBT gap region and decays away from the nano-gap region. The tail of electrical field into the silicon layer is longer than that into the silver layer. Its reason is due to the lossless Si layer compared with the lossy Ag metal layer. The electrical field distributions *E*y of the fundamental TM mode of the NWHPW in the middle of the DDMEBT layer along the *y*- and *x*-axis, respectively, are demonstrated in line graphs, in Fig. 2.

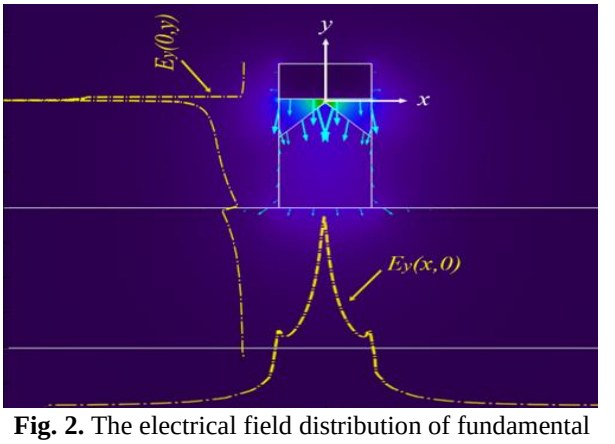

Fig. 2. The electrical field distribution of fundamental TM mode in the investigated NWHPW. The thicknesses of DDMEBT and silver were assumed to be h_gap=10nm and h_Ag=110nm, respectively and α=45°.Ey(0, y) and Ey(x, 0) are 1D y-component of electrical field distribution.

3. KERR NONLINEAR ANALYSIS

The electrical field in the waveguide is governed by the following equation [18]

$$\nabla^2\vec{\boldsymbol{E}} - \frac{1}{c^2}\frac{\partial^2\vec{\boldsymbol{E}}}{\partial t^2} = \mu_0\frac{\partial^2\vec{\boldsymbol{P}}_L}{\partial t^2} + \mu_0\frac{\partial^2\vec{\boldsymbol{P}}_{NL}}{\partial t^2} \quad (1)$$

where the linear and nonlinear polarization components ($\vec{\boldsymbol{P}}_L, \vec{\boldsymbol{P}}_{NL}$) are related to the electrical field $\vec{\boldsymbol{E}}$ by

$$\vec{\boldsymbol{P}}_L(\vec{r},t) = \varepsilon_0\chi^{(1)}\vec{\boldsymbol{E}}(\vec{r},t) \quad (2)$$

$$\vec{\boldsymbol{P}}_{NL}(\vec{r},t) = \varepsilon_0\chi^{(3)}\vec{\boldsymbol{E}}(\vec{r},t)\vec{\boldsymbol{E}}(\vec{r},t)\vec{\boldsymbol{E}}(\vec{r},t) \quad (3)$$

respectively. Where, ε_0 is the free space permittivity, $\chi^{(1)}$ is the linear susceptibility, and $\chi^{(3)}$ is the nonlinear susceptibility tensor.

The influence of $\chi^{(3)}$ makes the effective refractive index dependent on the optical intensity *I*

$$n(\omega, I) = n_0(\omega) + n_2 I \quad (4)$$

where n_2 is the optical Kerr coefficient. Taking into account that

$$I = \frac{\langle |E|^2 \rangle_{\mathrm{t}}}{Z} \quad (5)$$

where $Z = \sqrt{\mu_0/\varepsilon_0\varepsilon_{\mathrm{r}}}$ is the so-called wave impedance, μ_0 is the vacuum permeability, $\langle . \rangle_{\mathrm{t}}$ stands for a time average operator, where the spectrum of linear refractive index $n_0(\omega)$ is straightforwardly referring to the spectrum of linear optical susceptibility $\chi^{(1)}(\omega)$

$$n_0^2(\omega) = 1 + \chi^{(1)}(\omega) \quad (6)$$

and it also can be expressed via the well-known Sellmeier approximation [19, 20]. Nonlinear index coefficient n_2 and third-order susceptibility $\chi^{(3)}$ are related as $n_2 = 3\mathrm{Re}\left[\chi^{(3)}\right]/4\varepsilon_0\, cn^2$[21].

The Kerr nonlinear coefficient γ in a passive waveguides is often utilized to determine the nonlinearity as [22]:

$$\gamma = \frac{2\pi\overline{n_2}}{\lambda A_{\mathrm{eff}}} \quad (7)$$

where λ is the optical wavelength in free space, $\overline{n_2}$ is the nonlinear refractive index averaged over an inhomogeneous cross-section weighted concerning electric and magnetic field distribution, and A_{eff} is the effective mode area defiend as [22]:

$$\overline{n_2} = \frac{\varepsilon_0 \iint n_0^2(x,y) n_2(x,y) \left[2\left|\vec{\boldsymbol{E}}\right|^4 + \left|\vec{\boldsymbol{E}}^2\right|^2\right] dA}{\mu_0 \quad 3\iint \left|\left(\vec{\boldsymbol{E}} \times \vec{\boldsymbol{H}}^*\right).\hat{z}\right|^2 dA} \quad (8)$$

$$A_{\mathrm{eff}} = \frac{\left|\iint (\mathbf{E} \times \mathbf{H}^*).\hat{z}\, dA\right|^2}{\iint |(\mathbf{E} \times \mathbf{H}^*).\hat{z}|^2\, dA} \quad (9)$$

where $n_0(x,y)$ and $n_2(x,y)$ are the linear and nonlinear refractive index distribution within the cross-section, respectively.

As demonstrated recently in ref. [23, 24], a new FoM was defined including propagation length, optical damage threshold power, and confinement factor as well as the Kerr nonlinear coefficient suitable to characterize the Kerr nonlinear performance of hybrid plasmonic waveguides. This Fig. of merit simultaneously quantifies the optical loss, optical mode confinement, and the degree of Kerr nonlinearity, defined as:

$$\mathrm{FoM} = L_{\mathrm{P}} P_{0,\mathrm{th}} \gamma = L_{\mathrm{P}} P_{0,\mathrm{th}} \sum_{i=1}^{m} (\gamma_i\, \Gamma_i) \quad (10)$$

Where Γ_i is

$$\Gamma_i = \frac{\iint_{A_i} \frac{1}{2} Re\{(\mathbf{E} \times \mathbf{H}^*).\hat{z}\}\, dA}{\iint_{A_{tot}} \frac{1}{2} Re\{(\mathbf{E} \times \mathbf{H}^*).\hat{z}\}\, dA} \quad (11)$$

$P_{0,\mathrm{th}} = A_{\mathrm{eff}}^{\mathrm{P}} I_{\mathrm{th}}$ is an optical damage threshold for the polymer, where $A_{\mathrm{eff}}^{\mathrm{P}} = P_{\mathrm{mode}}/c\varepsilon_0 n_{\mathrm{m}} \max\{|E_{\mathrm{loc}}|^2\}/2$, beyond this value, the polymer will get damaged [25]. I_{th} is a DDMEBT polymer property and assumed $I_{\mathrm{th}} = 5\ \mathrm{GWcm^{-2}}$ [26].

4. KERR NONLINEAR SIMULATION RESULTS AND DISCUSSION

This section mainly deals with the parametric study of NWHPW and its various modal characteristic and Kerr nonlinear performance such as effective mode area, propagation length, and confinement factor of the fundamental mode, nonlinear coefficient, and FoM. We can control the guiding performance of a waveguide by using the geometric parameters. The guiding performance of the NWHPW was evaluated as a function of height (h_{gap}), width (W), and angle (α) as indicated in Fig. 1.

The confinement factor of the fundamental mode of the proposed NWHPW for DDMEBT layer and triangle part of Si layer as a function of wedge angles (α) with $h_{\mathrm{gap}} = 10\mathrm{nm}$ and $W = 200\mathrm{nm}$ are indicated in Fig. 3. The confinement factor of the DDMEBT layer increases until reaches the maximum value of $\Gamma_{\mathrm{DDMEBT}} = 0.33$ for $\alpha = 35°$. In comparison with results of $\Gamma_{\mathrm{DDMEBT}} = 0.22$ obtained in ref. [24], we can observe a higher degree of confinement than in the planar interface (i.e. $\Gamma_{\mathrm{DDMEBT}} = 0.33$). Therefore, there are large differences between the Kerr nonlinear characteristics of the NWHPW and the planar HPW. An important difference between the previous HPWs [27] and the proposed structure is the modal confinement in the NWHPW structure. As shown in Fig. 2, the NWHPW concentrates the electrical fields on top of the

triangle tip, which causes large optical field enhancements due to small gap size. The electrical field is perpendicular to the Ag surface and the NWHPW mode is predominantly transverse magnetic (TM) polarized at the top of the triangle.

Fig. 4(a) shows the propagation length versus angle α in the range of 5° to 65°. The propagation length diminishes for smaller α angles because energy is localized in the wider polymer area which can lead to more loss due to more contact area with silver. By increasing α, the propagation length becomes in general much longer than the planar structure for a fixed $h_{\text{gap}} = 10\text{nm}$ and $W = 200\text{nm}$ [23]. Moreover, increasing the optical field confinement for $\alpha \approx 35°$ (see Fig. 3(a)), leads to stronger electrical field, so allows lower $P_{0,\text{th}}$ and vice versa.

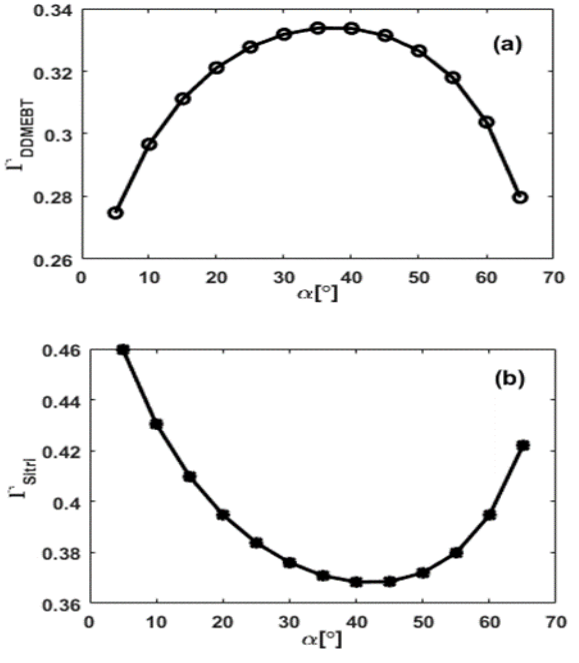

Fig. 3. (a)Confinement factor Γ of DDMEBT layer (b) and triangle tip part of silicon region versus α with $W = 200\text{nm}$ and $h_{\text{gap}} = 10$ nm.

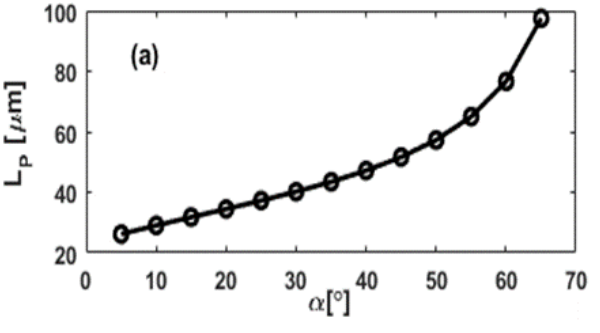

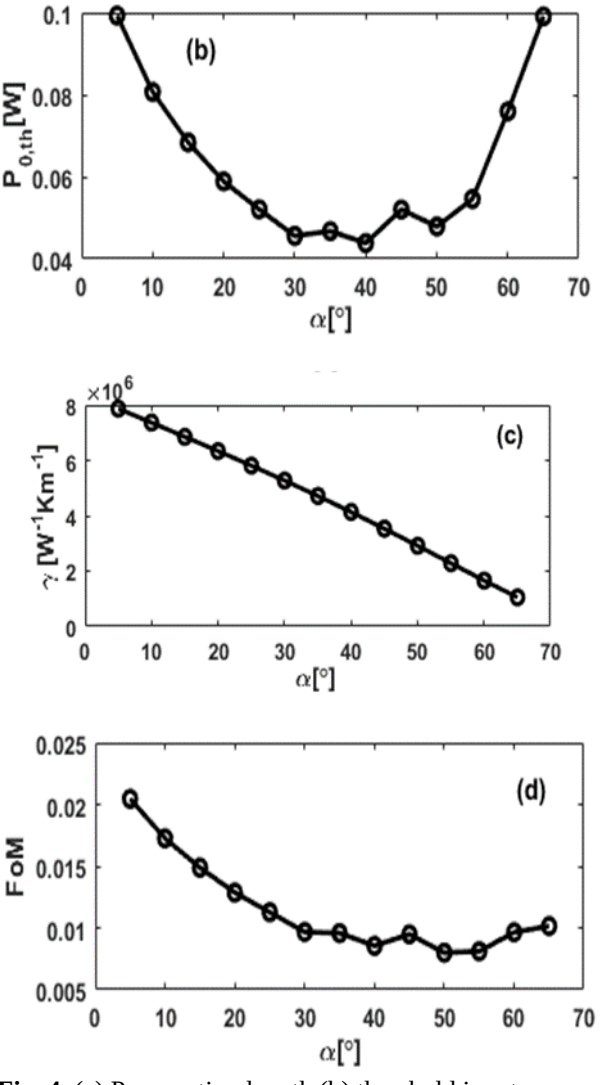

Fig. 4. (a) Propagation length (b) threshold input power (c) nonlinear coefficient γ, and (d) FoM as a function of angle.

For evaluating Kerr nonlinearity, we calculated the nonlinear coefficient γ by considering the nonlinearity of the DDMEBT layer and ignoring the nonlinear effect of rest layers due to less nonlinear refractive index order, as shown in Fig. 4(c). By increasing angle α, the effective mode area (A_{eff}) becomes larger, which leads to a weaker nonlinear coefficient γ (see eq. 7). In Fig. 4(d), the FoM was determined as a function of angle α. We observe that FoM of the NWHPW decreases with increasing α for $\alpha < 35°$ but is higher than that of the planar HPW [23]. Our results show that by increasing α , the propagation length can be improved, but Kerr nonlinear performance will be higher if we choose the ridge angle as small as possible. For $h_{\text{gap}} = 10\text{nm}, W = 200\text{nm}$ and $\alpha = 5°$, the minimum effective mode area $A_{\text{eff}} = 0.0263\mu\text{m}^2$ and maximum FoM $= 0.0058$ can be achieved.

Fig. 5(a) depicts the consequence of a change in the waveguide width Won the confinement factor Γ at $h_{\text{gap}} = 10\text{nm}$ and $\alpha = 45°$ for all layers. We can see that the confinement factors of the DDMEBT and triangle region Si are very close within range of $50\text{nm} < W < 200\text{nm}$. For $W > 200\text{nm}$, a larger portion of the optical mode is confined to the triangular silicon region. Fig. 5(b) shows the averaged nonlinear refractive indices $\overline{n_2}$of all layers as functions of W. In this case when $W > 550\text{nm}$, the value of $\overline{n_{2\text{Si}-\text{tri}}}$ become larger than $\overline{n_{2\text{DDMEBT}}}$. Therefore, we should notice for a relatively large size width, Kerr nonlinear performance is affected by all nonlinear layers, and considering all layers in simulations is necessary.

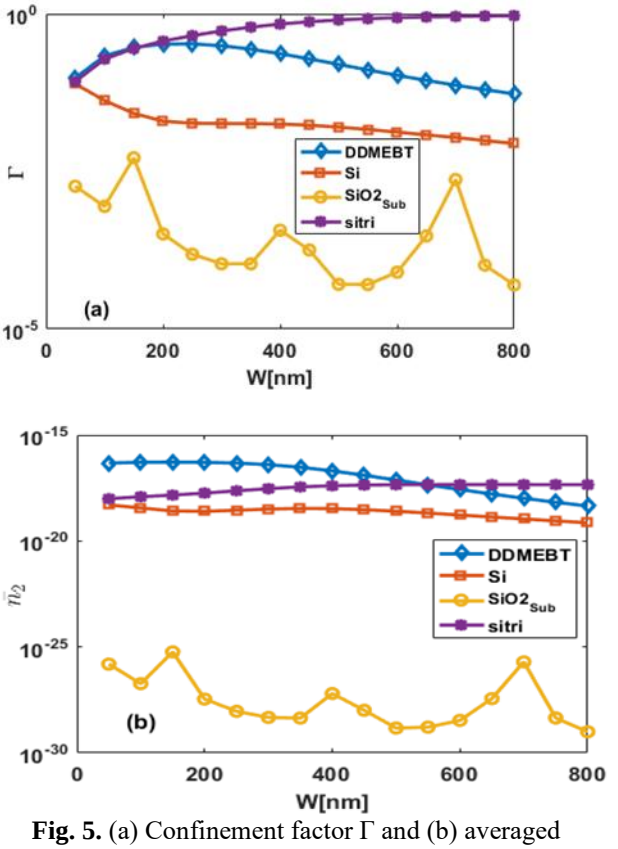

Fig. 5. (a) Confinement factor Γ and (b) averaged nonlinear refractive index for NWHPW versus W and h_gap=10 nm, α=45°.

Similarly, the variation of the overall nonlinear coefficient γ, which $\gamma = \sum_{i=1}^{m}(\gamma_i\, \Gamma_i)$, as a function of W is shown in Fig. 6(a) for $h_{\text{gap}} = 10$ nm and $\alpha = 45°$. It shows that the overall nonlinear coefficient reaches the maximum value of $\gamma = 1.35 \times 10^6 \text{W}^{-1}\text{Km}^{-1}$ at $W = 150$ nm. The Fig. of merit of the NWHPW is shown in Fig. 6(b). We can see FoM increases when the width increases. The comparison with the reported results in ref. [23, 24], NWHPW showed a better Kerr nonlinear performance rather than flat surface SOI-based and InP-based nonlinear HPW.

In Fig. 7(a) and (b), we have plotted the normalized effective mode area and propagation length, respectively, with different thicknesses of DDMEBT (h_{gap}) at W = 200 nm and $\alpha = 45°$. Here we start with the $h_{\text{gap}} = 10\text{nm}$ and vary it upto 200 nm. At $h_{\text{gap}} = 10\text{nm}$, larger propagation length of $L_{\text{p}} = 51\mu\text{m}$ is obtained with minimum effective mode area of $A_{\text{eff}} = 0.0586\mu\text{m}^2$, which is comparable to other structures reported in ref. [23]. Fig. 7(c) depicts the increase of $P_{0,\text{th}}$ due to less confinement of the optical field. By considering Fig. 7(d), it can be understood that $\overline{n_2}$ of other layers are negligible in comparison with the DDMEBT layer.

The maximum value of the nonlinear coefficient is obtained $\gamma = 3.53 \times 10^6 \text{W}^{-1}\text{Km}^{-1}$at $h_{\text{gap}} = 10\text{nm}$. Moreover, as we increase the thickness of the nonlinear polymer, nonlinearity decreases, and the mode area increases (see fig. 7(e)). Fig. 7(f) shows the FoM as ad function of h_{gap}. We observe that FoM increases rapidly from 0.0094 to around 0.0774, as h_{gap}increases from 10 nm to 200 nm, which shows better Kerr nonlinear performance in comparison with ref. [23].

5. CONCLUSION

The hybrid plasmonic waveguide is found to be superior in terms of low loss and nano-scale confinement in comparison with other types of hybrid plasmonic waveguides. In this paper, we have studied the Kerr nonlinearity of a different nonlinear wedge-shaped hybrid plasmonic waveguide and compared it with the flat surface hybrid plasmonic waveguide published in the current literature. For such purpose, we utilized the finite element method to calculate the electromagnetic fields and refractive index of the investigated waveguide. Then we obtained the Kerr nonlinear parameters for a nonlinear wedge-shaped hybrid plasmonic waveguide.

The proposed structure with a gap filled with DDMEBT material gives high mode confinement inside the gap and high propagation length. The confinement of the fundamental mode with DDMEBT gap gives minimum effective mode area $A_{\text{eff}} = 0.0586\mu\text{m}^2$ and large propagation length $L_{\text{p}} = 51\mu\text{m}$ for the certain value of wedge angle, waveguide width and height of the DDMEBT layer. The nonlinear coefficient for $h_{\text{gap}} = 10\text{nm}$ is $\gamma = 3.53 \times 10^6 \text{W}^{-1}\text{Km}^{-1}$. The proposed nonlinear waveguide is suitable for SOI-based photonic integrated platform.

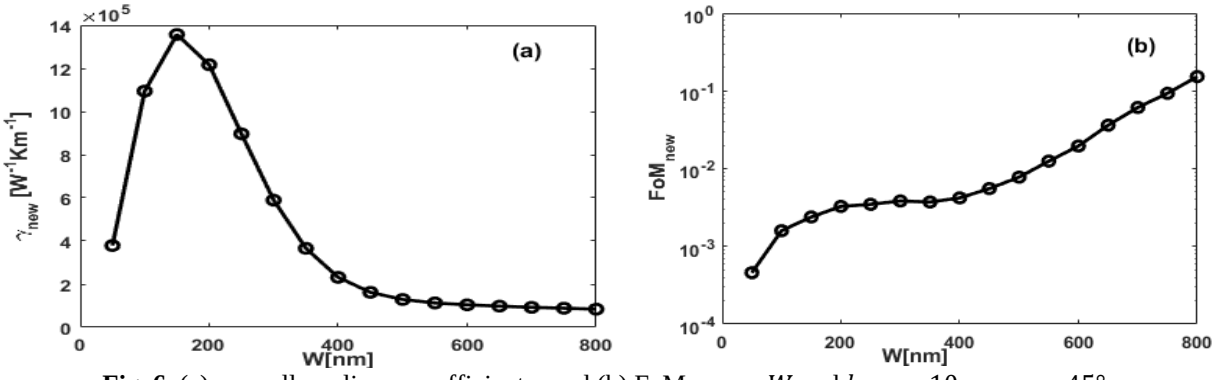

Fig. 6. (a). overall nonlinear coefficient γ and (b) FoM versus W and $h_{\text{gap}} = 10$ nm, $\alpha = 45°$.

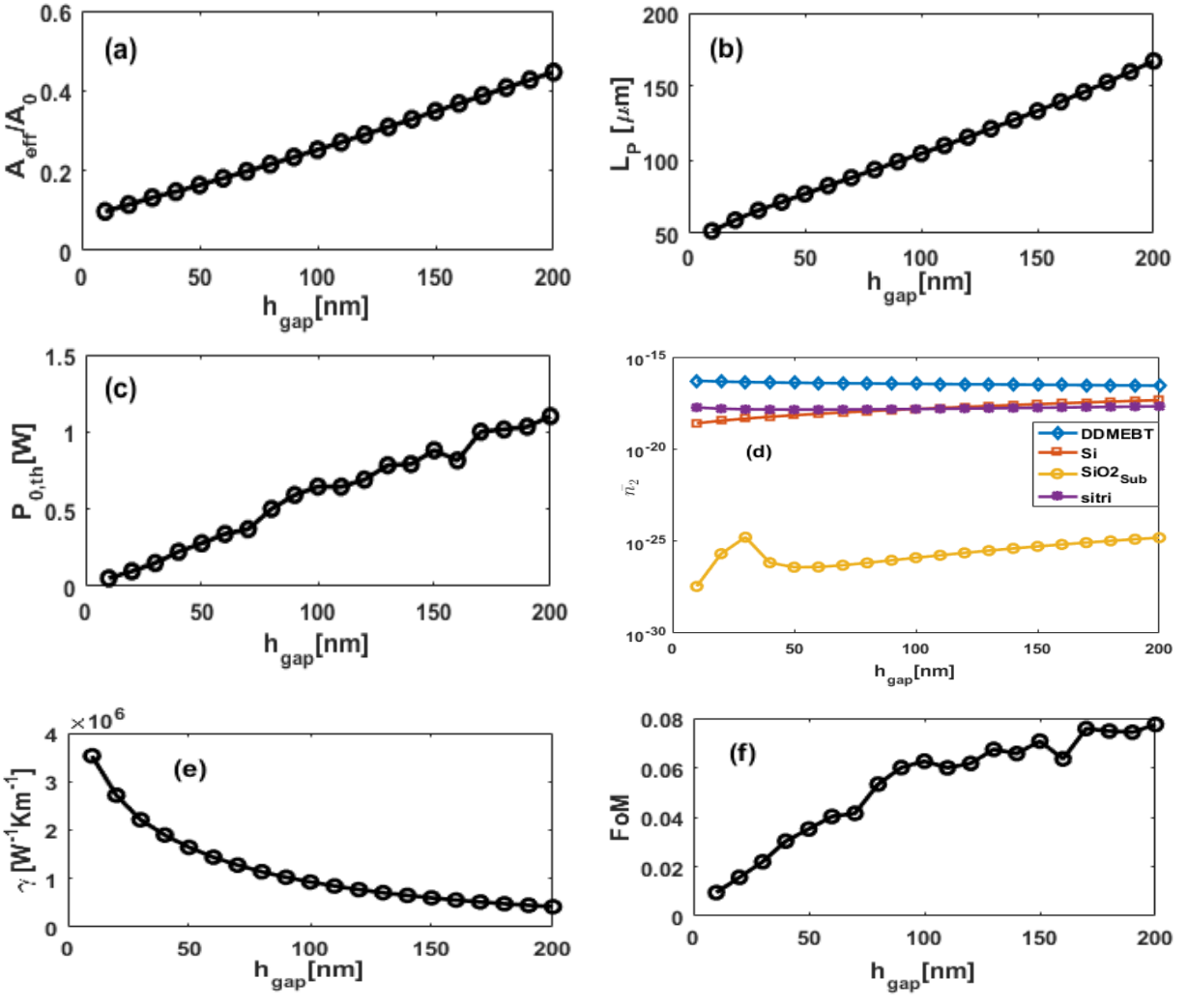

Fig. 7. (a) Normalized mode area, (b) propagation length,(c) threshold input power, (d) averaged nonlinear refractive index$\overline{n_2}$,(e) nonlinear coefficient γ, and (f) FoM as a function of the DDMEBT layer thickness(h_{gap}) and $W = 200$nm and $\alpha = 45°$.

REFERENCES

[1] Oulton RF, Sorger VJ, Genov DA, Pile DF, Zhang X. "**A hybrid plasmonic waveguide for subwavelength confinement and long-range propagation".** *nature photonics*. 2008 Aug;2(8):496-500.

[2] Dai D, He S. **"A silicon-based hybrid plasmonic waveguide with a metal cap for a nano-scale light confinement"**. *Optics express*. 2009 Sep 14;17(19):16646-53.

[3] Wu M, Han Z, Van V. **"Conductor-gap-silicon plasmonic waveguides and passive components at subwavelength scale"**. *Optics Express*. 2010 May 24;18(11):11728-36.

[4] Sutherland RL. Handbook of *nonlinear optics* second edition, revised and expanded. OPTICAL ENGINEERING-NEW YORK-MARCEL DEKKER INCORPORATED-. 2003;82.

[5] Kauranen M, Zayats AV. **"Nonlinear plasmonics".** *Nat Photonics* 6 (11): 737–748.

[6] Barnes WL. **"Surface plasmon–polariton length scales": a route to sub-wavelength optics**. *Journal of optics A: pure and applied optics.* 2006 Mar 21;8(4):S87.

[7] Kumar S, Kumar P, Ranjan R. **"A metal-cap wedge shape hybrid plasmonic waveguide for nano-scale light confinement and long propagation rang".** *Plasmonics*. 2022 Feb;17(1):95-105.

[8] Pile DF, Ogawa T, Gramotnev DK, Okamoto T, Haraguchi M, Fukui M, Matsuo S. **"Theoretical and experimental investigation of strongly localized plasmons on triangular metal wedges for subwavelength waveguiding".** *Applied Physics Letters*. 2005 Aug 8;87(6):061106.

[9] Boltasseva A, Volkov VS, Nielsen RB, Moreno E, Rodrigo SG, Bozhevolnyi SI. **"Triangular metal wedges for subwavelength plasmon-polariton guiding at telecom wavelengths"** *Optics express*. 2008 Apr 14;16(8):5252-60.

[10] Moreno E, Rodrigo SG, Bozhevolnyi SI, Martín-Moreno L, García-Vidal FJ. "**Guiding and focusing of electromagnetic fields with wedge plasmon polaritons"**. *Physical review letters*. 2008 Jan 14;100(2):023901.

[11] Diaz FJ, Li G, de Sterke CM, Kuhlmey BT, Palomba S. **"Kerr effect in hybrid plasmonic waveguides".** *JOSA B*. 2016 May 1;33(5):957-62.

[12] Zhong Q, Fourkas JT. **"Optical Kerr effect spectroscopy of simple liquids".** *The Journal of Physical Chemistry B*. 2008 Dec 11;112(49):15529-39.

[13] Baehr-Jones TW, Hochberg MJ. **"Polymer silicon hybrid systems: A platform for practical nonlinear optics".** *The Journal of Physical Chemistry C*. 2008 May 29;112(21):8085-90.

[14] Enami Y, Derose CT, Mathine D, Loychik C, Greenlee C, Norwood RA, Kim TD, Luo J, Tian Y, Jen AY, Peyghambarian N. **"Hybrid polymer/sol–gel waveguide modulators with exceptionally large electro–optic coefficients".** *Nature Photonics*. 2007 Mar;1(3):180-5.

[15] Johnson PB, Christy RW. "**Optical constants of the noble metals".** *Physical review B*. 1972 Dec 15;6(12):4370.

[16] Johnson PB, Christy RW. **"Optical constants of the noble metals"**. *Physical review B*. 1972 Dec 15;6(12):4370.

[17] Lin Q, Zhang J, Piredda G, Boyd RW, Fauchet PM, Agrawal GP. **"Dispersion of silicon nonlinearities in the near infrared region."** *Applied physics letters*. 2007 Jul 9;91(2):021111.

[18] Agrawal GP. Nonlinear fiber optics: its history and recent progress. *JOSA B*. 2011 Dec 1;28(12):A1-0.

[19] Zhu J, Ozdemir SK, Xiao YF, Li L, He L, Chen DR, Yang L. **"On-chip single nanoparticle detection and sizing by mode splitting in an ultrahigh-Q microresonator".** *Nature photonics*. 2010 Jan;4(1):46-9.

[20] Arnold S, Keng D, Shopova SI, Holler S, Zurawsky W, Vollmer F. **"Whispering gallery mode carousel–a photonic mechanism for enhanced nanoparticle detection in biosensing".** *Optics Express. 2009* Apr 13;17(8):6230-8.

[21] Leuthold J, Freude W, Brosi JM, Baets R, Dumon P, Biaggio I, Scimeca ML, Diederich F, Frank B, Koos C. **"Silicon organic hybrid technology—A platform for practical nonlinear optics."** *Proceedings of the IEEE*. 2009 Jun 16;97(7):1304-16.

[22] Afshar S, Monro TM. **"A full vectorial model for pulse propagation in emerging waveguides with subwavelength structures part I: Kerr nonlinearity".** *Optics express*. 2009 Feb 16;17(4):2298-318.

[23] Li G, de Sterke CM, Palomba S. Fig. of **"merit for Kerr nonlinear plasmonic waveguides"**. *Laser & Photonics Reviews*. 2016 Jul;10(4):639-46.

[24] Firouzabadi MD, Nikoufard M, Tavakoli MB. **"Modifying the Fig. of merit in hybrid plasmonic waveguide for Kerr nonlinear effect".** *Indian Journal of Physics*. 2020 May;94(5):713-8.

[25] Afshar VS, Monro TM, de Sterke CM. **"Understanding the contribution of mode area and slow light to the effective Kerr nonlinearity of waveguides."** *Optics express*. 2013 Jul 29;21(15):18558-71.

[26] Li G, de Sterke CM, Palomba S. **"Performance comparison of Kerr nonlinear plasmonic waveguide configurations"**. InBragg Gratings, Photosensitivity, and Poling in Glass Waveguides. *Optical Society of America* 2016 Sep 5 (pp. JM6A-20)..

[27] Chu HS, Bai P, Li EP, Hoefer WR. **"Hybrid dielectric-loaded plasmonic waveguide-based power splitter and ring resonator: compact size and high optical performance for nanophotonic circuits".** *Plasmonics*. 2011 Sep;6(3):591-7.